Reaction of Alanine Racemase with 1-Aminoethylphosphonic Acid Forms a Stable External Aldimine[†,‡]

C. Geoffrey F. Stamper,[§] Anthony A. Morollo,[||] and Dagmar Ringe*[,||,⊥]

Program in Biophysics and Structural Biology, Departments of Biochemistry and Chemistry, and Rosenstiel Basic Medical Sciences Research Center, Brandeis University, Waltham, Massachusetts 02254

Received March 25, 1998; Revised Manuscript Received May 27, 1998

ABSTRACT: (*R*)-1-Aminoethylphosphonic acid (L-Ala-P), a synthetic L-alanine analogue, has antibacterial activity and is a time-dependent inactivator of all purified Gram-positive bacterial alanine racemases that have been tested. L-Ala-P forms an external aldimine with the bound pyridoxal 5′-phosphate (PLP) cofactor, but is neither racemized nor efficiently hydrolyzed. To understand the structural basis of the inactivation of the enzyme by L-Ala-P, we determined the crystal structure of the complex between L-Ala-P and alanine racemase at 1.6 Å resolution. The cofactor derivative in the inhibited structure tilts outward from the protein approximately 20° relative to the internal aldimine. The phosphonate oxygens are within hydrogen bonding distance of four amino acid residues and two water molecules in the active site of the enzyme. L-Ala-P is an effective inhibitor of alanine racemase because, upon formation of the external aldimine, the phosphonate group interacts with putative catalytic residues, thereby rendering them unavailable for catalysis. Furthermore, this aldimine appears to be inappropriately aligned for efficient Cα proton abstraction. The combination of these effects leads to a stable aldimine derivative and potent inactivation of alanine racemase by this compound.

Alanine racemase is a pyridoxal 5′-phosphate (PLP[1])-dependent enzyme that catalyzes the isomerization between the L and D isomers of the amino acid alanine. In the L to D direction, the enzyme provides the D-alanine required in the synthesis of uridine diphosphate (UDP)-*N*-acetylmuramyl pentapeptide, a critical component of the bacterial cell wall. Because this pathway is unique to bacteria, alanine racemase has been an attractive target for antibacterial design.

Phosphonopeptides and aminophosphonates are effective inhibitors for peptidases (*1*), proteases (*2*, *3*), and lipases (*4*). Allen and co-workers, using alaphosphin (*5*), were the first to demonstrate the antibacterial activity of these types of compounds. Alaphosphin (L-alanyl-L-1-aminoethylphosphonic acid) is readily transported by bacterial cell wall permeases and then hydrolyzed by intracellular aminopeptidases to L-alanine (**1**) and (*R*)-1-aminoethylphosphonic acid (L-Ala-P, **2**).

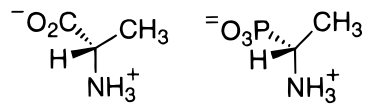

1 **2**

The bactericidal activity arises from the inhibition of alanine racemase by L-Ala-P. Ala-P competitively inhibits alanine racemase activity in crude extracts from Gram-negative bacteria (*Escherichia coli* and *Salmonella typhimurium*) and is a time-dependent and irreversible inactivator of alanine racemases from Gram-positive bacterial sources (*Streptomyces aureus* and *Streptococcus faecalis*) (*6*). The time-dependent inactivation has since been confirmed with purified enzymes from *S. faecalis* and the Gram-positive *Bacillus stearothermophilus*. The *S. faecalis* enzyme showed a rapid time-dependent loss of activity by both isomers of Ala-P (*7*). A more complete study of the inactivation of the highly purified *B. stearothermophilus* enzyme showed that L-Ala-P was inactivated in a time-dependent manner with an apparent K_i of 1 μM (*8*).

Spectroscopic analysis (*8*) and solid-state NMR experiments conducted by Copié and co-workers (*9*) demonstrated that L-Ala-P forms an external aldimine with the enzyme at C4′ on the PLP cofactor. The external aldimine, however, was neither racemized nor efficiently hydrolyzed and found to have a remarkably long half-life, estimated to be 25 days (*8*). It has not been established whether the limited reactivation occurs via hydrolysis of the aldimine or exchange of the derivative for fresh cofactor.

Phosphonates have multiple ionization states. At pH 6.0, 50% of the Ala-P in solution is the free acid (*10*). Badet

[†] This work was supported by a grant from the National Science Foundation (D.R.), in part by a grant from the Lucille P. Markey Charitable Trust, and in part by the Macromolecular Structure and Mechanism training grant from the National Institutes of Health (G.F.S.).

[‡] The coordinates for the complex have been deposited at the Brookhaven Protein Data Bank and are available under access code 1bd0.

* Corresponding author.

[§] Program in Biophysics and Structural Biology.

[||] Departments of Biochemistry and Chemistry.

[⊥] Rosensteil Basic Medical Sciences Research Center.

[1] Abbreviations: PLP, pyridoxal 5′-phosphate; L-Ala-P, (*R*)-1-aminoethylphosphonic acid; Tris, tris(hydroxymethyl)aminomethane; PEG 4K, poly(ethylene glycol) 4000 (molecular mass of 3.5−4.5 kDa); L-Ala-P−PLP, Schiff base formed between L-Ala-P and PLP. The use of a prime after an amino acid (e.g., Tyr265′) denotes a residue from the other subunit of the enzyme.

S0006-2960(98)00692-8 CCC: $15.00
Published on Web 06/26/1998

and co-workers (*8*) demonstrated that neither the monomethyl- or dimethylphosphonate derivatives of L-Ala-P are inhibitors of the *B. stearothermophilus* enzyme. On the basis of these results, they have suggested that the dianionic form of the phosphonate may sufficiently mimic a potential transition-state intermediate of the reaction, the aci form of the substrate−PLP carbanion, and the two negative charges are crucial for the observed inhibitory activity of L-Ala-P.

The recent determination of the crystal structure of the dimeric *B. stearothermophilus* alanine racemase (*11*) has made it possible to examine the structural basis for the inactivation. We report here the crystal structure of the L-Ala-P−PLP−enzyme complex at 1.6 Å resolution. Examination of the complex confirms that the inhibitor forms an external aldimine with the PLP cofactor. This cofactor derivative can be interpreted as an analogue of the external aldimine formed between substrate and enzyme; however, the enzyme is not able to racemize L-Ala-P or regenerate the internal aldimine efficiently because of critical interactions between the inhibitor and active site residues. We demonstrate here that the effectiveness of L-Ala-P as an inhibitor of the enzyme is not due to any resemblance of the aldimine derivative to a possible transition state but is due solely to the interactions it makes with the enzyme through the phosphonate group.

EXPERIMENTAL PROCEDURES

Materials. L-Ala-P and PEG 4K were purchased from Fluka Chemie AG (Buchs, Switzerland). The inhibitor was used as a 400 mM sodium salt stock solution prepared by titrating the dissolved free acid with 1 M NaOH to neutrality.

Protein Purification. B. stearothermophilus alanine racemase was prepared as described previously (*11*). The purified enzyme was dialyzed against 1 L of 100 mM Tris-HCl buffer (pH 8.5) and 10 μM PLP. The protein was then concentrated to 40 mg/mL using Amicon concentrators with a 10 kDa molecular mass cutoff.

Crystallization. A solution containing 40 mg/mL enzyme was diluted with the L-Ala-P salt solution to a final concentration of 30 mg/mL enzyme and 4 mM L-Ala-P. The crystals (0.7 mm × 0.7 mm × 0.3 mm) were grown by the hanging drop method. The hanging drop contained 10 μL of the inhibited protein solution, 10 μL of 21% (w/v) PEG 4K, 200 mM sodium acetate, and 100 mM Tris (pH 8.5). Drops were equilibrated against 700 μL of the PEG 4K solution. As described previously (*11*), the crystals have a distinct yellow color due to the presence of PLP in an aldimine linkage. The crystals belong to space group $P2_12_12_1$ with the following unit cell dimensions: $a = 98.23$ Å, $b = 87.69$ Å, $c = 85.30$ Å, and $\alpha = \beta = \gamma = 90°$. There is one dimer in the asymmetric unit.

Data Collection and Processing. Crystals of the complex between enzyme and the L-Ala-P−PLP aldimine were coated with oil and flash-cooled in liquid propane for data collection. One entire data set was collected from a single crystal kept frozen at 95 K by an Oxford Cryostream cooling device. The X-ray data were collected at the Brookhaven National Laboratory in the Biology Department single-crystal diffraction facility at beamline X12-C in the National Synchrotron Light Source using synchrotron radiation at a wavelength of 1.15 Å. The diffraction patterns were recorded using a CCD-based detector developed at Brandeis University by Phillips and co-workers (*12*). All diffraction data were integrated, scaled, and merged using the HKL software package, resulting in 97 731 unique reflections to a limit of 1.6 Å (*13*). Data processing results and refinement statistics are outlined in Table 1. The data beyond 1.8 Å are weak, with $I_{avg}/\sigma(I)_{avg}$ approaching 1.0. The outermost shell (resolution range of 1.66−1.6 Å) includes very weak reflections ($I_{avg} = 19.5$, $error_{avg} = 24.6$) where only 8% of the reflections were measured more than three times. In fact, there was no R_{merge} value reported for this resolution shell by the Scalepack program. However, χ^2 analysis indicated the errors on the measurements in the shells beyond 1.8 Å were properly estimated. Given the size of the shells and how poorly the reflections were measured, we were not that surprised by the increasingly higher R_{merge} values in the outer shells. Ultimately, the decision to keep all of the data was based on the quality of the final electron density maps where all data were included.

Table 1: Data and Refinement Statistics

Data Collection	
resolution range (Å)	25−1.6
no. of observations	516 378
no. of unique reflections $[I/\sigma(I) > 0]$	97 731
R_{merge} (%)[a]	7.8
completeness, overall (%)	96.7
completeness, outer shell (1.66−1.60 Å; %)	93.7
Model Refinement	
resolution range $[F/\sigma(F) > 0$; Å]	10−1.6
no. of reflections	80 258
R-factor[b] (%)	24.0
R-free (for 2505 reflections; %)	26.6
no. of protein atoms	6043
no. of L-Ala-P−PLP atoms	44
no. of water molecules	389
B-factor model	individual
rmsd from ideality	
bond lengths (Å)	0.01
bond angles (deg)	1.24
improper angles (deg)	0.71
dihedral angles (deg)	26.3

[a] $R_{merge} = \Sigma|I_{obs} - I_{avg}|/\Sigma I_{avg}$. [b] $R\text{-factor} = \Sigma||F_{obs}| - |F_{calc}||/\Sigma|F_{obs}|$, where F_{obs} is the observed structure factor amplitude and F_{calc} is the calculated structure factor amplitude.

Structure Solution and Refinement. Since the crystal of the inhibitor−enzyme complex was nearly isomorphous with that of the structure reported by Shaw et al. (*11*), the native structure as a dimer was used as the starting model. To remove the native structure model bias, the PLP cofactor, acetate, and water molecules were removed from the original coordinate file (access code 1SFT) prior to refinement. All refinement procedures were carried out using the software package X-PLOR (*14*). A total of 2505 reflections were used for free *R*-factor calculations, in which subsets of the data (3%) were omitted from the refinement for testing purposes (*15*).

Application of phases calculated from the original coordinates resulted in an initial crystallographic *R*-factor of 0.39 and a free *R*-factor of 0.41. The starting model was then subjected to rigid body refinement using reflections in the 20−4.0 Å resolution range (6000 reflections). This procedure lowered the crystallographic *R*-factor to 0.33 and the

Scheme 1: Racemization Reaction Catalyzed by Alanine Racemase[a]

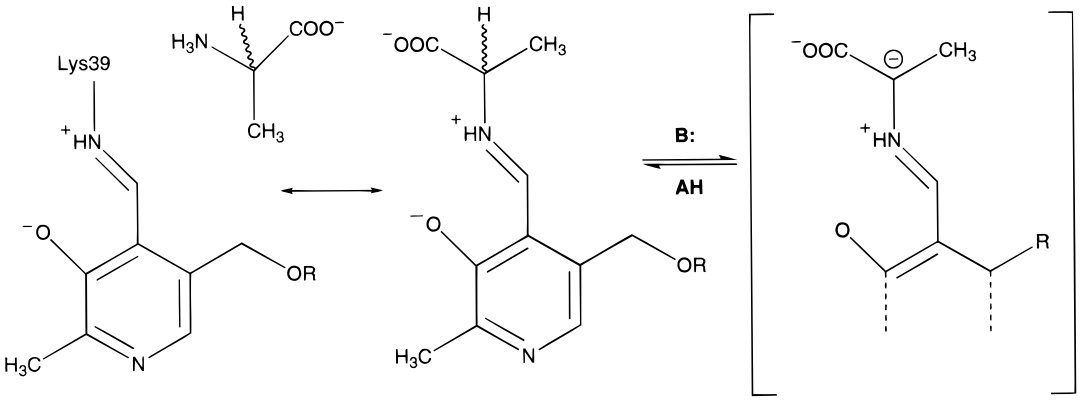

[a] The stereochemistry of the incoming substrate is left ambiguous, signifying that both isomers of alanine are substrates. The α-carbanion is in brackets, indicating that the transition state of the reaction is presently unknown.

free *R*-factor to 0.33. Subsequent rounds of positional refinement were carried out by incrementally including higher-resolution data and fewer lower-resolution reflections. The final positional refinement procedure used all of the reflections in the resolution range of 10.0−1.6 Å (80 258 reflections). This round of refinement gave an overall *R*-factor of 0.32 and an *R*-free of 0.37. Difference electron density maps with coefficients $2F_{obs} - F_{calc}$ and $F_{obs} - F_{calc}$ (*16*, *17*) were calculated at this stage in the refinement, providing interpretable electron density for a covalent cofactor derivative in the active site. A model of the cofactor derivative was built using the program QUANTA (Molecular Simulations, Inc.), and the coordinates were added to the protein model. A total of 112 water molecules that were observed in the original native structure (1SFT) and whose electron density was observed at these positions in the current structure were added to the model. This new model was then subjected to further rounds of positional refinement as well as overall and individual *B*-factor refinement procedures.

Additional water molecules were added to the model using the WATERPICK procedure in the X-PLOR program package. The final model includes a total of 389 water molecules and two L-Ala-P−PLP aldimines, one per active site. The final *R*-factor for all reflections in the 10−1.6 Å resolution range is 0.24 with a free *R*-factor of 0.26. Refinement and model quality statistics are summarized in Table 1. The decision to include the data out to 1.6 Å resolution was based on the quality of the observed electron density maps. There were obvious improvements in areas of the electron density when all the data were used in the calculation of the maps. Refinement with data to 1.9 Å resolution ($R_{merge} = 0.23$, $I_{avg}/\sigma(I)_{avg} = 4.1$) using data where $F/\sigma(F) > 2.0$ did result in an improved *R*-factor (0.21); however, equally substantial improvements were not observed in the calculated electron density maps. Analysis of the protein using PROCHECK showed that 90.2% of all the residues were in the most favored regions of a Ramachandran plot, 9.1% of the residues were in additional allowed regions, and 0.7% of the residues were in generously allowed regions.

A series of simulated annealing omit maps (*18*), in which 30 residues were systematically omitted throughout the entire chain of each monomer, were calculated to elucidate large conformational changes or rearrangements in the overall fold. No such distortions were found. There is interpretable electron density for most of the structure; however, there are surface residues where the side chain density is poor or absent.

RESULTS AND DISCUSSION

The racemization of alanine by alanine racemase represents the simplest reaction catalyzed by a class of enzymes that utilize PLP as a cofactor. This reaction requires an initial transaldimination reaction, in which the Schiff base between the PLP and Lys39, the internal aldimine, is displaced by the amino group of the substrate forming an external aldimine. Deprotonation of the α-carbon and reprotonation of the stabilized α-carbanion then leads to formation of the other enantiomer (Scheme 1). Product is released via the reverse transaldimination reaction, which regenerates the internal aldimine. L-Ala-P is a mechanism-based inhibitor of alanine racemase that forms an external aldimine with the PLP cofactor (*9*). L-Ala-P seems to follow the same initial steps of the reaction as the substrate does. Indeed, the structure reported here shows a covalently linked L-Ala-P−PLP aldimine, demonstrating the ability of L-Ala-P, like substrate, to displace Lys39 via transaldimination to form this intermediate. The structure of the L-Ala-P−PLP−enzyme complex affords us the opportunity to explain why L-Ala-P is a good inhibitor of alanine racemase and, in particular, allows us to predict specific residues that may be involved in the reaction mechanism of the enzyme. Further, closer examination of this structure should provide evidence of any conformational changes that might occur in the enzyme during formation of an external aldimine, the first step of the racemization reaction.

Comparison of the Overall Fold with That of the Native Structure. We have determined the structure of the L-Ala-P−PLP−enzyme complex to 1.6 Å resolution and compared it to the native structure (*11*). In forming the external aldimine, the protein does not undergo any major conformational changes. The rms deviations between the native (*11*) and inhibited structures are 0.32 (Cα) and 0.59 Å (all non-hydrogen atoms). The larger rms deviations in side chain positions may to some extent reflect differences in conformations of surface residues between data collected at room temperature, as was the case for the native structure, and the data collected at 95 K in the current report.

The important differences in the structure occur in the active site. The side chains of a number of active site

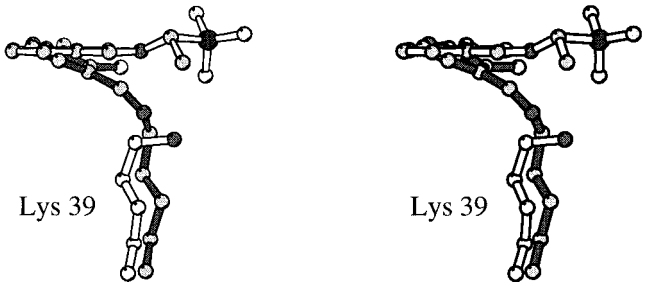

FIGURE 1: Stereodiagram of the L-Ala-P−PLP aldimine (in white) overlaid with the internal aldimine reported by Shaw (in black; *11*) viewed from the side, with the PLP phosphates removed for clarity. The angle between the planes of the pyridine rings is approximately 20°. The active site lysine (Lys39) of the L-Ala-P−PLP aldimine structure is included (in white).

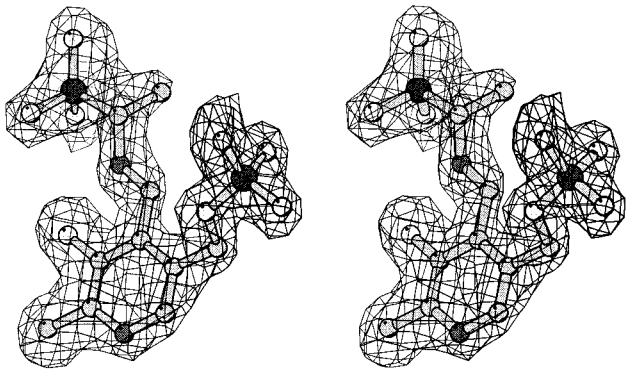

FIGURE 2: Stereodiagram of the L-Ala-P−PLP aldimine as it appears in the active site of the enzyme. The electron density shown was calculated using a simulated annealing omit map with coefficients $2F_{obs} - F_{calc}$ contoured at 1σ for which all the atoms shown were excluded from the calculation.

residues (Lys39, Tyr265′, and Arg136) have shifted position due to the presence of the cofactor derivative. The most important of these, Lys39, which is involved in a Schiff base with the PLP in the native structure, is now pointed away from the cofactor. In addition, the cofactor derivative has tilted away from the protein by approximately 20° relative to the native enzyme (Figure 1). A number of other active site residues have shifted slightly to accommodate the tilt of the cofactor.

Active Site. The electron density in the active site of the enzyme can only be interpreted as an external aldimine formed between L-Ala-P and the PLP cofactor (Figure 2). Further, the average *B*-factor for the aldimine derivative is 14.7 Å^2 compared to the average *B*-factor for the protein (21.6 Å^2), indicating that there is one fully occupied cofactor derivative per active site. The electron density of the aldimine derivative has no connectivity to any residue on the protein in the active site. A model of the aldimine derivative formed between the PLP cofactor and L-Ala-P fits perfectly into the observed density.

The electron density of the aldimine derivative is planar from N1 of the PLP through the imine linkage. The α-carbon of the phosphonate is not in the plane of the ring, and the electron density about the carbon suggests sp^3 geometry. Initially, the geometry of the α-carbon was refined using ideal sp^3 geometric restraints. Then the restraints were relaxed, yielding final angles about the α-carbon of 108, 100, and 110°, respectively, suggesting that the α-carbon is still protonated. The only configuration of the alanine portion of the model that fits the density is the L-isomer since there is clear electron density for both the methyl and phosphonate groups. The position of the phosphonate group is well defined with individual lobes of electron density for each oxygen atom. There is little or no evidence for the presence of the D-isomer of Ala-P in the electron density of simulated annealing omit maps in which all the atoms of the aldimine derivative were removed (Figure 2). These results suggest that there has been little or no racemization of L-Ala-P in this complex. A number of experiments have been reported to test whether Cα−H cleavage occurs for complexes between alanine racemase and this inhibitor. No Cα−H cleavage is observed when α-tritio-D,L-Ala-P is incubated with both the *S. faecalis* and the *B. stearothermophilus* enzymes (*7*, *8*). There is more than adequate space in the active site immediately around the methyl group of L-Ala-P to accommodate it. The only protein atoms close by are those of the side chain of Met312′. If this structure were the D-isomer, with the phosphonate group bound in the same way, the methyl group would be solvent-exposed. Therefore, there is no obvious structural reason this enzyme is so specific for alanine as substrate.

The L-Ala-P−PLP aldimine is held in the active site by a network of hydrogen bonds (Figure 3) similar to those found in the native structure (*11*). The active site is solvent accessible and includes many water molecules. Many of the interactions in the hydrogen-bonding network involve interactions with the phosphonate group of the inhibitor. One oxygen of the inhibitor, O8, interacts with the NZ of the Lys39 side chain (2.9 Å) and a water molecule (wat132, 2.6 Å). The lysine side chain now points away from the cofactor and is interacting with the side chain of a residue from the other subunit, Asp313′. A second oxygen from the phosphonate (O6) forms a hydrogen bond (2.8 Å) with the backbone amide of Met312′ and an active site water molecule (wat124, 2.5 Å). A similar interaction with the backbone amide of Met312′ is also found in the native structure where a bound acetate molecule is presumed to bind like substrate (*11*). The third oxygen on the phosphonate (O7) is interacting with Tyr265′ (2.6 Å) and Arg136 (2.6 Å). In addition to the interaction with the O7 phosphonate oxygen, Arg136 forms a hydrogen bond with the phenolic oxygen (3.0 Å) on the PLP cofactor. This is the only interaction in the active site where a single residue on the enzyme is interacting with both the cofactor and the inhibitor.

On the basis of an acetate molecule bound in the active site of the native structure, Shaw et al. (*11*) described which interactions might be important for binding and positioning of substrate. In the native structure, the carboxylate moiety of the acetate molecule forms a hydrogen bond with both the backbone amide of Met312′ and the guanidinium group of Arg136 (*11*). Our structure shows these same two interactions with the phosphonate group of L-Ala-P; however, we observe two additional interactions for L-Ala-P, with the phenolic oxygen of Tyr265′ and the NZ of Lys39. Although L-Ala-P is not a substrate, the phosphonate moiety is, in part, positioned in the active site by the same two interactions that position the carboxylate group of acetate. Further, the L-Ala-P makes these two interactions as part of an external aldimine with the PLP cofactor. This suggests that L-Ala-P is a good model for understanding substrate binding and underlies the importance of the backbone amide of Met312′

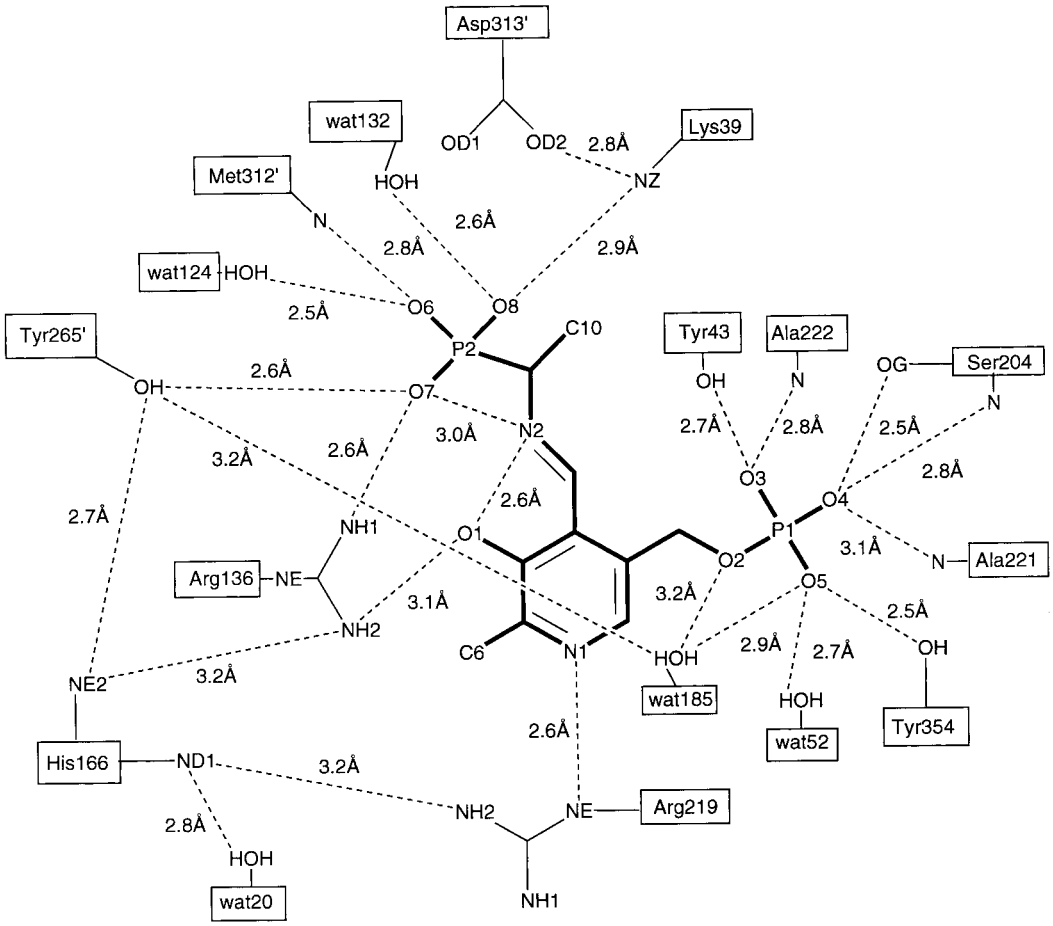

FIGURE 3: Schematic diagram showing the interactions between the L-Ala-P−PLP aldimine and the amino acid residues and water molecules in the active site of the enzyme. For clarity, only the atoms of the side chains involved in the interactions are included. Atoms are labeled in PDB format.

and the side chain of Arg136 in the recognition of the substrate by the enzyme. In addition, Arg136 makes a hydrogen bond with the phenolic oxygen of the PLP cofactor, an interaction that may also be important for positioning substrate relative to the cofactor.

It has been suggested that the effectiveness of dianionic L-Ala-P as an inhibitor of alanine racemase is due to its resemblance to an aci form of a carbanion; delocalization of the electron pair of the α-carbanion onto the carboxylate of substrate as a possible transition state for the reaction (*8*). The inability of both the monomethyl- and dimethylphosphonate derivatives to inhibit the enzyme leads to the prediction that the dianion is critical for the inhibitory activity (*7*). Our structure indicates that the lack of inhibition observed with these two L-Ala-P esters may be due to either steric repulsion or a loss of critical binding interactions provided by the oxygens on the phosphonate. It appears from the structure that the active site could not even accommodate the monomethyl derivative. Further, the structure indicates no obvious preference for a di- or monoanionic species. The reported pK_a's for L-Ala-P in solution would suggest that it is dianionic at pH 8.5 (*10*), and we have modeled it as such. Our conclusion is that, upon formation of the external aldimine, the additional interactions the phosphonate moiety makes with active site residues due to the presence of the third oxygen are the critical components of the observed inhibition. In fact, as previously mentioned, there are at least two additional interactions with the enzyme compared to carboxylate groups bound in a similar way (*11*; A. A. Morollo, unpublished results). Although we believe the L-Ala-P−PLP aldimine is analogous to a substrate external aldimine, it does not seem to resemble a possible transition state of the reaction catalyzed by the enzyme.

Proton Abstraction and Racemization. The next step in the mechanism of the racemization reaction after formation of the external aldimine is deprotonation of the α-carbon. In our current structure, the α-carbon of the phosphonate is clearly in the *R*-configuration, which is derived from the L-isomer of Ala-P, indicating that proton abstraction has not occurred. The stability of the L-Ala-P−PLP aldimine affords us the opportunity to look for the active site residue(s) that would ordinarily catalyze removal of the Cα proton. It has been shown for L-aspartate aminotransferase that deprotonation at the α-carbon is catalyzed by the active site lysine (Lys258 in the *E. coli* enzyme) that forms the internal aldimine in the native enzyme (*19*). It is assumed, therefore, that the equivalent lysine (Lys39) is capable of acting as a base in the reaction catalyzed by alanine racemase. However, in the configuration that we observe in the structure of this cofactor derivative, the Cα proton must be pointing away from Lys39. Furthermore, Lys39 is interacting with both the carboxylate group of Asp313′ and O8 on the phosphonate. In addition, the NZ of Lys39 is 4.1 Å from the α-carbon of the phosphonate. At this distance, it could not act directly as a base. Since Lys39 is interacting with two

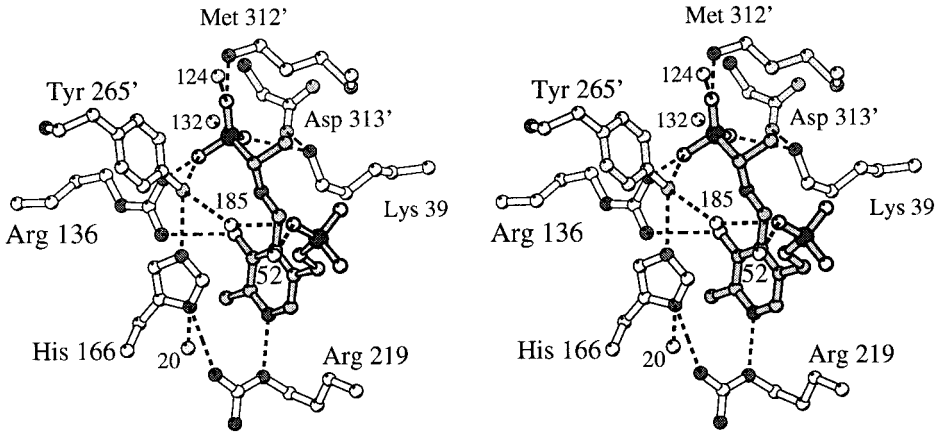

FIGURE 4: Stereodiagram of the L-Ala-P−PLP aldimine and the active site residues and water molecules that directly interact with it. The dashed lines indicate putative hydrogen bonds of ≤3.2 Å. The active site water molecules are labeled by their numbers as found in the PDB file.

negatively or partially negatively charged atoms, it is reasonable to suggest that, even if Lys39 were in position to act as the general base, these interactions would prevent it.

Sawada (*20*), on the basis of kinetic evidence, and Shaw (*11*), on the basis of structural evidence, have both proposed that the racemization reaction catalyzed by alanine racemase requires two bases. Indeed, our structure shows that Tyr265′ is 3.2 Å from the α-carbon, in position to act as a general base (see Figure 4). It has been reported that the equivalent tyrosine in the *E. coli* enzyme, acting as a nucleophile, was responsible for the mechanism-based inhibition by 3-halovinylglycine (*21*). If the racemization of alanine is catalyzed via a two-base mechanism, then Tyr265′ would be the likely candidate for a second base (*11*). According to our structure, it appears that this residue, while in position to act as a base, does not in this case. This may be due to the types of interactions with which the phenolic oxygen of Tyr265′ is involved. This oxygen is within hydrogen bonding distance of His166 (2.7 Å), O7 of the phosphonate (2.6 Å), and an active site water molecule (wat185) not observed in the native structure (3.2 Å). One possible explanation for the lack of α-proton abstraction by Tyr265′ is the hydrogen bond that the phenolic oxygen makes with O7 of the phosphonate group. This interaction could prevent Tyr265′ from acting as a general base despite its proximity to the α-carbon (3.2 Å). A similar observation was made in the crystal structure of chymotrypsin inactivated by 3-benzyl-6-chloro-2-pyrone. The structure of the complex showed that the active site histidine (His57) was interacting with a terminal carboxylate on the inhibitor, thereby rendering it unable to activate a water molecule required for deacylation (*22*).

PLP-dependent enzymes catalyze a larger variety of reactions than any other cofactor-dependent enzyme (*23*). According to the Dunathan hypothesis, the type of reaction catalyzed depends in part on the functional group held perpendicular to the plane made by the conjugated π system of the PLP ring and the α-carbon of the substrate (*24*). In the case of L-aspartate aminotransferase, there is good evidence that the Cα−H bond is held perpendicular to this π system (*25*, *26*). Modeling of external aldimines in the active site of dialkylglycine decarboxylase has also suggested that this hypothesis may hold true (*27*). During initial refinement of the structure reported here, the torsion angle about the Schiff base linkage between L-Ala-P and PLP was restrained to 0°, keeping the nitrogen in the plane of the ring as would be expected for an external aldimine. When these restraints were relaxed, the torsion angle remained at 0° and the observed electron density from N1 of the PLP through the imine linkage remained planar. Efficient proton abstraction then requires that the α-proton be held perpendicular to this conjugated system. In Figure 5, we have added the proton to the α-carbon of L-Ala-P, while maintaining the existing geometry, to see how the enzyme could orient this bond. This figure shows clearly that the α-carbon of L-Ala-P is not in the plane of the conjugated system and that the Cα−H bond is not perpendicular to it, thereby removing the potential for orbital overlap. A possible explanation for the unfavorable geometry in this complex for proton abstraction may be the additional interactions that the tetrahedral phosphonate moiety makes at the active site of the enzyme.

Product Release. Regenerating the internal aldimine, thereby releasing product, is the final step of the reaction. This step requires the attack of Lys39 at C4′ on the PLP. In our structure, the NZ of Lys39 is 4.3 Å from C4′ and, as previously mentioned, is involved in interactions with both a protein residue and an oxygen on the phosphonate. These interactions prevent Lys39 from acting as a nucleophile at C4′ of the imine linkage, thereby contributing to the unusually long half-life of the L-Ala-P−PLP aldimine.

An alternative explanation for the stability of the L-Ala-P−PLP aldimine has been proposed by Badet and co-workers (*8*). These workers attempted to reduce the L-Ala-P−PLP aldimine in the active site of the enzyme with excess sodium borohydride. Interestingly, they found that this excess of sodium borohydride was unable to reduce the L-Ala-P external aldimine chromophore. However, the same excess of sodium borohydride reduced both the internal aldimine of the native enzyme and the external aldimine formed between the enzyme and alanine, instantly. It was only upon denaturation of the L-Ala-P-inactivated enzyme that borohydride was able to gain access to the imine linkage (*8*). They interpreted these results as a conformational change in the enzyme upon binding of the inhibitor, which excludes water from the active site. In this structure, we observe no conformational changes upon inhibitor binding, and the active site is solvent accessible. Consequently, there is ample space in the active site for approach of the reducing agent. However, it has been demonstrated that small, unsubstituted

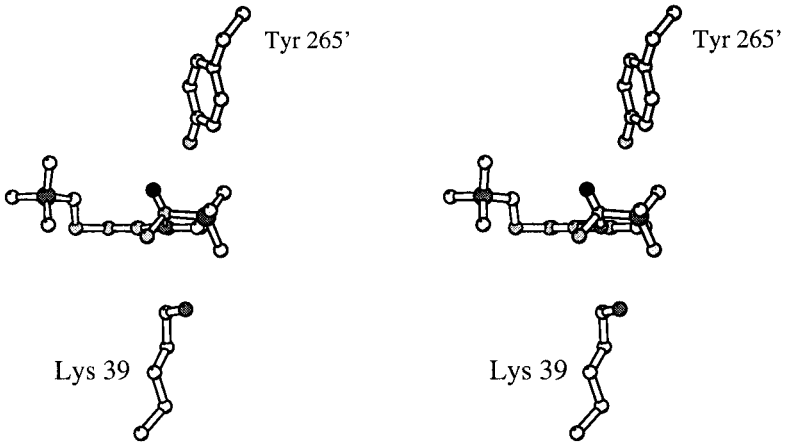

FIGURE 5: Stereodiagram of the L-Ala-P−PLP aldimine viewed perpendicular to the plane of the PLP ring. The black atom is a proton that has been modeled onto the α-carbon of L-Ala-P while maintaining the observed geometry about the α-carbon. The putative catalytic residues Tyr265′ and Lys39 are shown. This view shows clearly that the α-carbon is not in the plane of the PLP ring.

reducing reagents such as sodium borohydride preferentially attack carbon−nitrogen π bonds via an axial approach (*28*), and the lack of reactivity at the L-Ala-P−PLP imine linkage may be due to steric hindrance. According to our structure, the L-Ala-P−PLP aldimine is positioned in the active site such that an axial attack by borohydride should be possible, making this explanation unlikely.

Badet's results together with the structure reported here suggest that there is some characteristic about the imine linkage with L-Ala-P in the context of the active site that could prevent its reduction. Copié and co-workers observed a protonated nitrogen at pH 7.6 for the imine nitrogen in the L-Ala-P−PLP aldimine (*9*). We assume that the protonation state of the imine nitrogen in our structure is unchanged despite the pH difference between the two experiments (pH 8.5 in this experiment), on the basis of the types of interactions observed for this nitrogen atom. In our structure, the imine nitrogen is 2.6 Å from the phenolic oxygen on the PLP ring and 3.0 Å from both O7 and O8 of the phosphonate. These interactions support a positively charged imine nitrogen. For a substrate external aldimine, presumably, only the interaction with the phenolic oxygen on the PLP would be present. Therefore, differences in the electronic environment around the imine linkages of the L-Ala-P−PLP external aldimine, a substrate external aldimine, or the internal aldimine provide one possible explanation for the differences in their reactivity. This unique environment, however, is dependent on an intact active site of the enzyme since the L-Ala-P cofactor derivative is susceptible to reduction when the enzyme is denatured.

CONCLUSION

We report here the crystal structure of the L-Ala-P−PLP aldimine in complex with alanine racemase. This is the first structure of an external aldimine reported for the enzyme. The structure demonstrates that the effectiveness of this inhibitor, upon formation of the external aldimine, is due to specific interactions that the phosphonate moiety makes with putative catalytic residues in the active site. In addition, the tetrahedral geometry of the phosphonate positions the α-carbon of the L-Ala-P in a manner different than that expected for a productive substrate. In this position, the α-carbon is not in the plane of the PLP ring, which may make activation of the Cα−H σ bond more difficult. Thus, the enzyme appears to be "locked" as an unreactive external aldimine, leading to the unusually long half-life.

The structure of this complex also allows us to predict the roles of specific residues in the reaction mechanism of the racemase. Racemization requires both deprotonation and reprotonation from opposite sides of the same carbon atom. This structure of the L-Ala-P−PLP-enzyme complex, together with other experiments (*20*), supports a two-base mechanism for this process. If the overall reaction required only a single base (Lys39), consistent with other PLP enzymes that abstract an α-proton, then it becomes difficult to predict, on the basis of this structure, how Lys39 could reach the α-proton of L-alanine. It seems more reasonable to invoke a second base, Tyr265′, which is appropriately aligned for proton abstraction from an L-isomer in the active site of this structure. We predict that D-alanine would bind in the active site with the carboxylate positioned like the phosphonate group of L-Ala-P, but with the α-proton facing the opposite direction within reach of Lys39.

ACKNOWLEDGMENT

We thank Tracy Arakaki and Dr. Juan Carlos Amor for assistance with the data collection and Drs. Kenji Soda, Nobuyoshi Esaki, Liz Hedstrom, and Greg Petsko for helpful discussions. We also gratefully acknowledge the help of Dr. Robert M. Sweet and his staff at the Brookhaven National Laboratory in the Biology Department single-crystal diffraction facility at beamline X12-C in the National Synchrotron Light Source. The diffraction experiments reported in this paper were conducted with a CCD-based detector developed with a grant from the National Science Foundation (Grant NSFBIR-9321872) to Walter Phillips.

REFERENCES

1. Lambeir, A. M., Borloo, M., De Meester, I., Belyyaev, A., Augustyns, K., Hendriks, D., Scharpe, S., and Haemers, A. (1996) *Biochim. Biophys. Acta 1290*, 76−82.
2. Bertrand, J. A., Oleksyszyn, J., Kam, C. M., Boduszek, B., Presnell, S., Plaskon, R. R., Suddath, F. L., Powers, J. C., and Willams, L. D. (1996) *Biochemistry 35*, 3147−3155.
3. Charlton, J., Kirschenheuter, G. P., and Smith, D. (1997) *Biochemistry 36*, 3018−3026.

4. Stadler, P., Zandonella, G., Haalck, L., Spener, F., Hermetter, A., and Paltauf, F. (1996) *Biochim. Biophys. Acta 1304*, 229−244.
5. Allen, J. G., Atherton, F. R., Hall, M. J., Hassall, C. H., Holmes, S. W., Lambert, R. W., Nisbet, L. J., and Ringrose, P. S. (1978) *Nature 272*, 56−58.
6. Atherton, F. R., Hall, M. J., Hassall, C. H., Lambert, R. W., Lloyd, W. J., and Ringrose, P. S. (1979) *Antimicrob. Agents Chemother. 15*, 696−705.
7. Badet, B., and Walsh, C. T. (1985) *Biochemistry 24*, 1333−1341.
8. Badet, B., Inagaki, K., Soda, K., and Walsh, C. T. (1986) *Biochemistry 25*, 3275−3282.
9. Copié, V., Faraci, W. S., Walsh, C. T., and Griffin, R. G. (1988) *Biochemistry 27*, 4966−4970.
10. Wozniak, M., Nicole, J., and Tridot, G. (1972) *Bull. Soc. Chim. 11*, 4445−4452.
11. Shaw, J. P., Petsko, G. P., and Ringe, D. (1997) *Biochemistry 36*, 1329−1342.
12. Phillips, W., Stanton, M., O'Mara, D., and Li, Y. (1993) in *X-ray Detector Physics and Applications II*, pp 133−138, The International Society for Optical Engineering 2009, Bellingham, WA.
13. Otwinowski, W., and Minor, W. (1997) *Methods Enzymol. 276*, 307−326.
14. Brünger, A. T. (1996) *X-PLOR, A system for X-ray Crystallography and NMR*, Version 3.851, Yale University Press, New Haven, CT.
15. Brünger, A. T. (1992) *Nature 355*, 472−475.
16. Read, R. (1986) *Acta Crystallogr. A42*, 140−149.
17. Kleywegt, G. J., and Brünger, A. T. (1996) *Structure 4*, 897−904.
18. Hodel, A., Kim, S.-H., and Brünger A. T. (1992) *Acta Crystallogr. A48*, 851−859.
19. Julin, D. A., Wiesinger, H., Toney, M. D., and Kirsch, J. F. (1989) *Biochemistry 28*, 3815−3821.
20. Sawada, S., Tanaka, Y., Hayashi, S., Ryu, M., Hasegawa, T., Yukio, Y., Esaki, N., Soda, K., and Takahashi, S. (1994) *Biosci., Biotechnol., Biochem. 58*, 807−811.
21. Thornberry, N. A., Bull, H. G., Taub, D., Wilson, K. E., Giménez-Gallego, G., Rosegay, A., Soderman, D. D., and Patchett, A. A. (1991) *J. Biol. Chem. 266*, 21657−21665.
22. Ringe, D., Mottonen, J. M., Gelb, M. H., and Abeles, R. H. (1986) *Biochemistry 25*, 5633−5638.
23. John, R. A. (1995) *Biochim. Biophys. Acta 1248*, 81−96.
24. Dunathan, H. C. (1966) *Proc. Natl. Acad. Sci. U.S.A. 55*, 712−716.
25. Kirsch, J. F., Eichele, G., Ford, G. C., Vincent, M. G., and Jansonius, J. N. (1984) *J. Mol. Biol. 174*, 497−525.
26. Jäger, J., Moser, M., Sauder, U., and Jansonius, J. N. (1994) *J. Mol. Biol. 239*, 285−305.
27. Toney, M. D., Hohenester, E., Keller, J. W., and Jansonius, J. N. (1995) *J. Mol. Biol. 245*, 151−179.
28. Hutchins, R. O., Su, W., Sivakumar, R., Cistone, F., and Stercho, Y. P. (1983) *J. Org. Chem. 48*, 3412−3422.

BI980692S